Electronic structure and chemical bonding of divanadium-oxide clusters (V_2O_x, $x=3-7$) from anion photoelectron spectroscopy

Hua-Jin Zhai and Lai-Sheng Wang[a)]
Department of Physics, Washington State University, Richland, Washington 99352 and W. R. Wiley Environmental Molecular Sciences Laboratory, Pacific Northwest National Laboratory, Richland, Washington 99352

(Received 14 June 2002; accepted 7 August 2002)

We report a photoelectron spectroscopic investigation of a series of divanadium-oxide clusters $V_2O_x^-$ ($x=3-7$). Well-resolved spectra were obtained at three photon energies (355, 266, and 193 nm), revealing the structural and electronic evolution as the number of oxygen atoms increases in the cluster series. A behavior of sequential oxidation was observed in $V_2O_x^-$ for x up to 5: low binding energy features with primarily V $3d$ characters were disappearing in numbers and simultaneously shifting to higher binding energies with increasing oxygen content as a result of V→O charge transfers. Finally, for $V_2O_6^-$ and $V_2O_7^-$, the photoelectron spectra exhibit very-high-binding-energy features characteristic of O $2p$ characters. Vibrationally resolved spectra were obtained for the ground-state features of $V_2O_4^-$ and $V_2O_6^-$, with a spacing of 1090 cm^{-1} (V_2O_4) and 800 cm^{-1} (V_2O_6), which are assigned to V–O stretching vibrations. Electron affinities are reported for V_2O_3 to V_2O_7, and those of 5.61 eV for V_2O_6 and 5.38 eV for V_2O_7 are among the highest electronic affinities ever reported. The data are compared with previous theoretical calculations. © *2002 American Institute of Physics.* [DOI: 10.1063/1.1510441]

I. INTRODUCTION

Transition-metal oxides are of increasing importance in technological applications.[1] Vanadium oxides are commonly used in semiconductors, optical devices, and coatings.[1] They are also involved in many important industrial catalytic processes, from $SO_2 \rightarrow SO_3$ oxidation[2] to selective reduction of nitric oxide by ammonia.[3] However, microscopic details of such catalytic processes are still under debate.[4] Since a complex metal-oxide surface may be alternatively described as a collection of clusters with different sizes and isomers,[5] gas-phase studies of the electronic structure and chemical bonding of oxide clusters may provide a molecular-level understanding of such complex catalytic processes.

Indeed, extensive gas-phase studies have been performed on vanadium-oxide clusters during the past years. A number of mass spectrometric, collision-induced dissociation, photofragmentation, and reactivity studies by Castleman and co-workers[6–12] showed that VO_2, VO_3, and V_2O_5 units are the main building blocks for the oxygen-rich V_xO_y clusters. The growth mechanisms of neutral V_xO_y clusters were investigated by Foltin *et al.*[13] using covariance mapping time-of-flight mass spectrometry, which indicated that V_xO_y clusters grow from small V_2O or V_2O_3 clusters by the uptake of VO or VO_2 only. $V_xO_y^-$ anion clusters have also been observed,[11,12,14,15] and the formation enthalpies of several vanadium oxide anions, as well as the electron affinities of VO_2 and V_4O_{10}, have been determined.[14] Wu and Wang[16] reported a photoelectron spectroscopic study of the monovanadium-oxide cluster anion VO_x^- ($x=1-4$). Recently, Asmis *et al.*[17] reported infrared photodissociation spectra of a gas-phase $V_4O_{10}^+$ cation. Matrix electron spin resonance (ESR) and Fourier transform infrared (FTIR) studies were also conducted for monovanadium oxides and V_2O_2.[18,19] A number of recent theoretical studies have also been devoted to vanadium-oxide clusters.[20–24]

In the current article, we present a study on the electronic structure of a series of divanadium oxide clusters V_2O_x ($x=3-7$) using anion photoelectron spectroscopy (PES). This is a continuation of our research interest on oxide clusters.[16,25–32] Despite the previous works on vanadium-oxide clusters, little experimental spectroscopic information is available on these clusters. PES is a valuable technique to probe the electronic structure and chemical bonding of gas-phase clusters. In the current work, we report well-resolved PES data for divanadium-oxide clusters $V_2O_x^-$ ($x=3-7$). We observed that the vanadium $3d$-derived features dominated the low-binding-energy region of the PES spectra for $x=3-5$. The numbers of $3d$ features decrease and their binding energies increase with increasing oxygen content due to charge transfers from the metal to oxygen. A ''metal-nonmetal'' transition as indicated by a dramatic PES pattern change is shown between $V_2O_5^-$ and $V_2O_6^-$, and the PES spectra for the larger oxide clusters are characteristic of high-binding-energy features primarily of oxygen $2p$ character. The evolution of the PES spectral patterns and the measured electron affinities and vibrational information were interpreted by and compared with previous available theoretical calculations.[20–24]

II. EXPERIMENT

The experiment was carried out using a magnetic-bottle-type PES apparatus equipped with a laser vaporization super-

a)Electronic mail: ls.wang@pnl.gov

TABLE I. Observed electron affinities (EA's), vertical detachment energies (VDE's), and vibrational frequencies from the photoelectron spectra of $V_2O_x^-$ ($x=3-7$).[a]

	Obs. feature	EA (eV)	VDE (eV)	Vib. freq. (cm^{-1})
$V_2O_3^-$	*X*	1.76 (3)	2.05 (3)	
	A		2.38 (3)	
	B		2.76 (3)	
	C		~3.1	
$V_2O_4^-$	*X*	2.86 (2)	2.99 (2)	1090 (30)
	A		~4.8	
	B		5.55 (5)	
	C		5.90 (5)	
$V_2O_5^-$	*X*	3.99 (2)	4.31 (3)	
	A		~5.5	
	B		6.07 (2)	
$V_2O_6^-$	*X*	5.61 (3)	5.95 (5)	800 (40)
	A		6.32 (2)	
	X'	3.5 (1)	~4.2	
$V_2O_7^-$	*X*	5.38 (8)	~5.7	
	A		6.15 (5)	

[a]The numbers in parentheses represent the experimental uncertainty in the last digitals.

sonic cluster source, details of which have been described previously.[33,34] Briefly, the $V_xO_y^-$ cluster anions were produced by laser vaporization of a pure vanadium target in the presence of a helium carrier gas seeded with 0.5% O_2 or 1% N_2O. Various clusters were produced from the source and analyzed using a time-of-flight mass spectrometer. The $V_2O_x^-$ ($x=3-7$) species were each mass selected and decelerated before being photodetached. Three detachment photon energies were used in the current study: 355 nm (3.496 eV), 266 nm (4.661 eV), and 193 nm (6.424 eV). Photoelectrons were collected at nearly 100% efficiency by the magnetic bottle and analyzed in a 3.5-m-long electron flight tube. The photoelectron spectra were calibrated using the known spectrum of Rh^-, and the resolution of the apparatus was better than 30 meV for 1-eV electrons.

III. RESULTS

The obtained PES spectra for $V_2O_x^-$ ($x=3-7$) at different wavelengths are shown in Figs. 1–4. Under our current source conditions (helium carrier gas seeded with 0.5% O_2 or 1% N_2O), we found that it was difficult to produce the $V_2O_x^-$ ($x=0-2$) species with sufficient intensity for us to perform photodetachment experiments. This was likely because these oxygen-deficient species are too reactive with oxygen to survive in the source. The observed detachment transitions are labeled with letters, and the vertical lines represent the resolved vibrational structures. The obtained electron affinities (EA's), vertical binding energies (VDE's), and vibrational frequencies are summarized in Table I.

A. $V_2O_3^-$

The spectra of $V_2O_3^-$ were measured at three photon energies, as shown in Fig. 1. The 355-nm spectrum revealed a congested spectral pattern, indicating the high density of electronic states for the underlying neutral V_2O_3, for which we tentatively identified four spectral features (*X*, *A*, *B*, and *C*) with VDE's at 2.05, 2.38, 2.76, and ~3.1 eV, respectively.

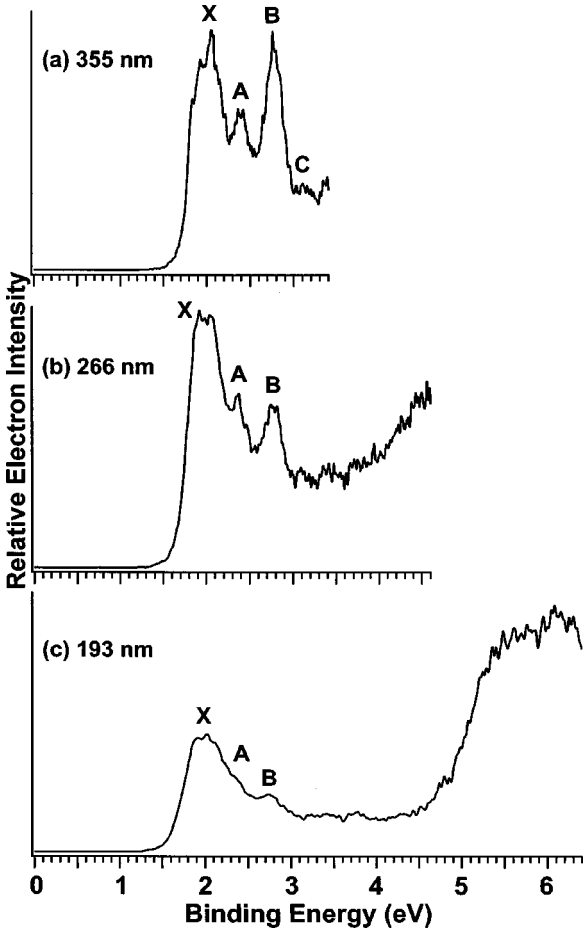

FIG. 1. Photoelectron spectra of $V_2O_3^-$ at (a) 355 nm (3.496 eV), (b) 266 nm (4.661 eV), and (c) 193 nm (6.424 eV).

Features *X* and *B* were fairly intense, whereas features *A* and *C* were relatively weak. Feature *X* displayed discernible fine structures, which could be due to either overlapping vibrational or electronic transitions. The onset of feature *X* defined an adiabatic detachment energy (ADE) of 1.76 eV, which also represented the EA of the neutral V_2O_3 species. Since no clear vibrational progressions were resolved for the *X* band, the EA was evaluated by drawing a straight line at the leading edge of the *X* band and adding a constant to the intersection with the binding energy axis to take into account the instrumental resolution and a finite thermal effect. The onset of the *X* band was sharp, allowing us to obtain a fairly accurate ADE. The 266-nm spectrum displayed continuous signals at the higher-binding-energy side [Fig. 1(b)], likely due to overlapping electronic transitions. The 193-nm spectrum again revealed continuous, but also intense, signals.

B. $V_2O_4^-$

The PES spectra of $V_2O_4^-$ (Fig. 2) were much simpler and better resolved than those of $V_2O_3^-$. The ground-state transition (*X*) displayed a simple vibrational progression with a spacing of 1090 cm^{-1}, which was clearly resolved in both the 355- and 266-nm spectra. The 0-0 transition defined an ADE of 2.86 eV for $V_2O_4^-$, which also represented the EA for the corresponding neutral V_2O_4 species. The VDE was

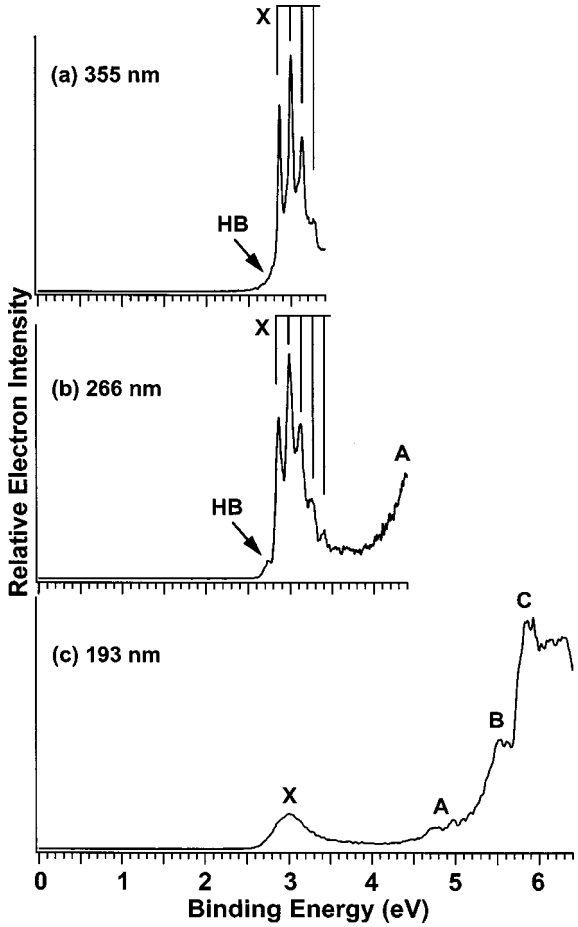

FIG. 2. Photoelectron spectra of $V_2O_4^-$ at (a) 355, (b) 266, and (c) 193 nm. The vertical lines represent vibrational structures. "HB" denotes a hot band transition.

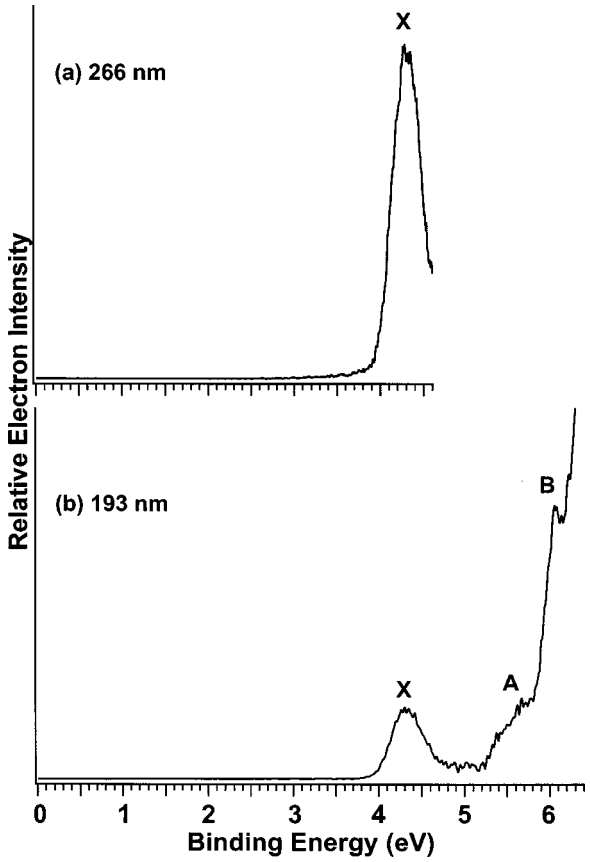

FIG. 3. Photoelectron spectra of $V_2O_5^-$ at (a) 266 and (b) 193 nm.

defined by the $1 \leftarrow 0$ transition at 2.99 eV. The weak feature at ~2.78 eV, labeled as HB in Fig. 2, was due to a hot band transition. The 266-nm spectrum did not reveal any additional features except the tail at the high-binding-energy side, indicating the onset of the *A* band. At 193 nm, a series of intense and broad spectral features were observed. The *A* band (~4.8 eV VDE) was weak and not well defined. At the higher-binding-energy side of the 193-nm spectrum, two more intense transitions were observed at VDE's of 5.55 eV (*B*) and 5.90 eV (*C*).

C. $V_2O_5^-$

$V_2O_5^-$ has much higher electron binding energies, and its PES spectra were recorded only at 266 and 193 nm, as shown in Fig. 3. At 266 nm, only one feature (*X*) was observed at a VDE of 4.31 eV. No vibrational structure was observed despite the rather high instrumental resolution provided at this energy range in the 266-nm spectrum (better than 30 meV). The relatively sharp onset of feature *X* defined an EA of 3.99 eV for the neutral V_2O_5 species. At 193 nm, two more features were observed at VDE's of ~5.5 eV (*A*) and 6.07 eV (*B*). The feature *A* was relatively broad and weak, whereas the feature *B* was sharp and intense.

D. $V_2O_6^-$ and $V_2O_7^-$

Due to their extremely high electron binding energies, only the 193-nm spectra could be recorded for $V_2O_6^-$ and $V_2O_7^-$. Figure 4(a) shows the spectrum for $V_2O_6^-$, which appeared to be rather different from those of the smaller $V_2O_x^-$ ($x \leqslant 5$) species. Two intense features (*X* and *A*) were observed at very high binding energies. The *X* band, which was assigned to the transition from the ground state of the $V_2O_6^-$ anion to the ground state of the V_2O_6 neutral, shows a partially resolved vibrational progression with a spacing of 800 cm^{-1}. The 0-0 transition defined an EA of 5.61 eV for the neutral V_2O_6 species, while the VDE of feature *X* was 5.95 eV. Feature *A* may represent the onset of a second band because its binding energy was close to the 193-nm photon energy. A VDE of 6.32 eV was obtained from the peak maximum. At the lower-binding-energy side of the $V_2O_6^-$ spectrum, broad and weak features were present. They slightly depended on the source conditions, but could not be completely eliminated. These features were attributed to the existence of a minor isomer. The feature X' as labeled appeared to be fairly well defined with an ADE of ~3.5 eV and a VDE of ~4.2 eV.

The 193-nm spectrum for $V_2O_7^-$ shown in Fig. 4(b) also revealed two intense features (*X* and *A*). The threshold feature (*X*) was relatively weak and broad with a VDE of ~5.7 eV. The onset of band *X* defined an EA of 5.38 eV for neutral V_2O_7, slightly lower than the EA of V_2O_6. The more intense *A* band has a VDE of 6.15 eV. Similar to $V_2O_6^-$, there

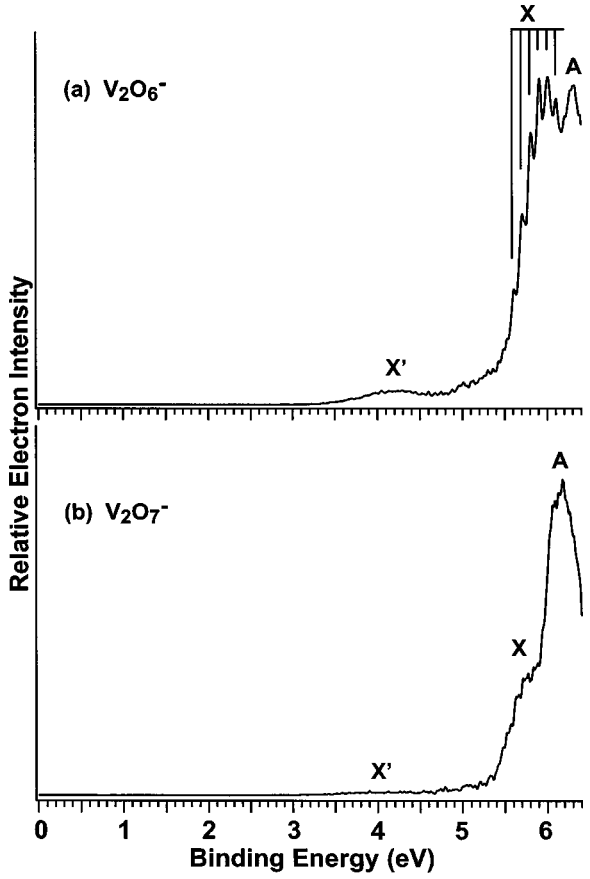

FIG. 4. Photoelectron spectra of (a) $V_2O_6^-$ and (b) $V_2O_7^-$ at 193 nm. The vertical lines represent vibrational structures.

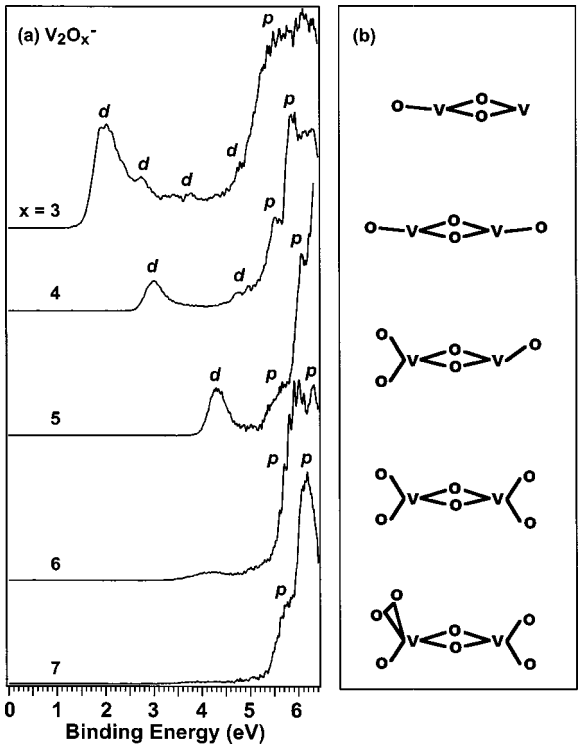

FIG. 5. (a) Comparison of the photoelectron spectra of $V_2O_x^-$ ($x=3-7$) at 193 nm. The observed electronic transitions are labeled as *d* or *p*, where *d* denotes photodetachment transitions from vanadium $3d$-derived orbitals and *p* denotes those from mainly oxygen $2p$-derived orbitals. (b) Schematic structures for V_2O_x and $V_2O_x^-$ based on available DFT calculations (Refs. 21–24).

existed a rather weak tail at the lower-binding-energy side of the spectrum [X' in Fig. 4(b)], which was also attributed to the existence of minor isomers.

IV. DISCUSSION

A. Comparison with previous calculations

The electron configuration of vanadium is $3d^34s^2$. It has four principal oxides in the bulk: VO, V_2O_3, V_2O_4, and V_2O_5, with oxidation states of the vanadium ranging from $+2$ to $+5$.[35] The chemical bonding between V and O in diatomic VO is extremely strong with both covalent and ionic characters.[36–39] In VO_x^- clusters, we showed previously that the V–O interactions involve strong ionic characters and their PES spectra can largely be elucidated on the base of simple electron counting.[16] For the divanadium-oxide clusters, recent density functional theory (DFT) calculations on various charge states (cation, neutral, and anion) from several research groups firmly established a key structural principle: i.e., in their ground state, all the V_2O_x and $V_2O_x^-$ species with $x\geqslant 2$ contain a doubly-oxygen-bridged four-membered ring unit, with the excess oxygen atoms terminally bonded to the vanadium atoms.[21–24] As will be shown below, chemical bonding in V_2O_x and $V_2O_x^-$ is also strongly ionic, and simple valence–electron counting is still valuable to understand their PES spectra and electronic structures: i.e., oxygen can be viewed as O^{2-} and the oxidation state of vanadium increases with increasing oxygen content until it is saturated at its highest possible oxidation state ($+5$). A similar picture was proposed in our previous works and was found to be highly useful to explain the electronic structural evolution for $Al_3O_x^-$ (Ref. 27) and $Fe_2O_x^-$ (Refs. 28 and 29) clusters, as well as for the monovanadium VO_x^- species.

In Fig. 5, we compare all the PES spectra of $V_2O_x^-$ ($x=3-7$) at 193 nm detachment photon energy. Schematic structures based on previous theoretical calculations[21–24] are also drawn in Fig. 5 to help elucidate the electronic and structural evolution of the $V_2O_x^-$ species. A detailed comparison of our PES data with *ab initio* calculations is given below.

1. $V_2O_3^-$

According to the DFT calculations by Calatayud *et al.*,[23] the ground state of neutral V_2O_3 possesses C_s symmetry, as shown schematically in Fig. 5(b). Two structures, one with a nonplanar ring ($^3A'$) and another with a planar ring ($^1A'$), were evaluated. The $^3A'$ state was found to be the ground state, with the $^1A'$ state 25.7 kcal/mol higher in energy. The $V_2O_3^-$ anion should possess either a quartet or doublet ground state, depending on which molecular orbital the extra electron occupies. However, no calculation is available for the $V_2O_3^-$ anion. Our PES spectra for $V_2O_3^-$ (Fig. 1) are the most complex and congested among all the oxide species reported here, indicating that there is a high density of low-lying electronic states for neutral V_2O_3. This is not surpris-

ing because of the unpaired $3d$ electrons in V_2O_3. The lower-binding-energy features (<5 eV) could then be assigned to detachment from the low-lying $3d$ electrons. The intense broad features beyond 5 eV were tentatively assigned to photodetachment from oxygen $2p$-derived orbitals. Further *ab initio* calculations seem to be warranted on $V_2O_3^-$ and V_2O_3 for a more detailed understanding of the electronic structure of these species.

2. $V_2O_4^-$

The ground-state structure of the neutral V_2O_4 cluster was predicted to be a four-membered ring with the two extra oxygen atoms each attached terminally to a vanadium atom [Fig. 5(b)].[21,23] It possesses C_{2v} symmetry with a triplet state ($^3B_2$). In V_2O_4 vanadium has a formal oxidation state of $+4$ (d^1) and the interaction between the d electrons of the two metal atoms is small, because there is little V–V bonding in the C_{2v} structure, resulting in the high spin coupling of the two unpaired d electrons on the two V centers. An open shell singlet of $^1A_2$ symmetry was also evaluated using the ''broken-symmetry'' approach, but was found to be higher in energy than the triplet state.[21,23] For the $V_2O_4^-$ anion, a high-spin $^4B_{2g}$ state with planar D_{2h} symmetry and an $(a_u)^1(a_g)^1(b_{2u})^1$ configuration was calculated to be the ground state at the B3LYP level of theory,[21] where the three unpaired electrons occupy bonding or antibonding d-type orbitals. Such a high-spin ground state would be expected to give rise to rather complicated PES spectrum upon photodetachment.

The PES spectra of $V_2O_4^-$ seemed to be rather simple (Fig. 2). However, there appeared to be weak and discernible signals in the entire low-binding energy range of the spectra between the X and A bands [Fig. 2(c)]. This suggested that there might be unresolved electronic states due to the excitations of the low-lying d electrons in this energy range, consistent with the open-shell nature of the V_2O_4 cluster. Thus we assigned the lower-energy features (<5 eV) to be due to the excitations of the $3d$ electrons and the higher-binding-energy features (B and C) to be due to detachment from O $2p$ orbitals.

3. $V_2O_5^-$

From simple valence-electron counting, a closed-shell ground state would be expected for neutral V_2O_5, in which all five valence electrons of V are transferred to O, and V reaches its highest oxidation state ($+5$). This is borne out from several previous DFT calculations.[21–23] The ground state of V_2O_5 was found to be a doubly bridged structure ($^1A_1$) as shown schematically in Fig. 5(b), where one vanadium atom has a tetrahedral coordination and the other has a trigonal-pyramidal coordination. Triply or singly bridged structures, in which both V atoms would have the same coordination environments, were calculated to be much higher in energy.[21–24] In its ground state, the terminal VO bonds in V_2O_5 are typical V=O double bonds, and the bridged VO bonds for the tetrahedrally coordinated vanadium atom are much longer than those for the trigonal-pyramidally coordinated vanadium.

The corresponding $V_2O_5^-$ anion was found to possess a similar doubly bridged structure with a $^2A'$ ground state. The highest occupied molecular orbital (HOMO) for the anion consists predominantly of the d_{z^2} orbital of the trigonal-pyramidally coordinated vanadium and has only very little contribution from the tetrahedrally coordinated vanadium $3d$ orbital or oxygen $2p$ orbitals. The electronic transitions from the open-shell $V_2O_5^-$ anion ground state to the closed-shell V_2O_5 neutral ground state and its low-lying excited states are expected to lead to a relatively simple PES pattern with a large energy gap, as was indeed observed (Fig. 3). The threshold PES feature (X) is well separated with feature A and is straightforwardly assigned to detachment of the unpaired electron from the anion d_{z^2} HOMO. The higher-binding-energy features (A and B) are assigned to be due to photodetachment of electrons from oxygen $2p$-derived orbitals.

4. $V_2O_6^-$

Further increasing the oxygen content beyond V_2O_5 would lead to ''oxygen-excessive'' species. The ground-state structures of V_2O_6 and $V_2O_6^-$ were similar, as schematically shown in Fig. 5(b). It is a doubly bridged structure with each vanadium atom terminally bonded to two oxygen atoms. The ground state for the corresponding $V_2O_6^-$ anion was predicted to be a doublet $^2B_{1u}$.[21] The singly occupied b_{1u} HOMO is found to delocalize over all six oxygen atoms, but with larger contributions from $2p$ orbitals of the terminal oxoligands. This is consistent with our PES spectrum [Fig. 5(a)], where a very high binding energy is revealed and a dramatic change in PES pattern is observed between $V_2O_6^-$ and the smaller $V_2O_x^-$ species. All the PES features observed for $V_2O_6^-$ should be due to detachment of electrons from oxygen $2p$-derived orbitals.

5. $V_2O_7^-$

V_2O_7 and $V_2O_7^-$ are even more ''oxygen-excessive'' species, and their ground-state structures were found to be similar to that of V_2O_6 and $V_2O_6^-$, except that one terminal oxygen atom is replaced by an O_2 unit,[21] as schematically shown in Fig. 5(b). V_2O_7 and $V_2O_7^-$ are hence the first species with a peroxoligand among the V_2O_x and $V_2O_x^-$ series. The anion ground state was found to be a doublet $^2A''$ state with C_s symmetry, whereas the neutral possesses a closed-shell $^1A'$ ground state.[21] The rather long VO bonds between vanadium and the two peroxo-oxygen atoms and the short OO bonds indicates a relatively weak metal-peroxide interaction, which may be partially responsible for the slight decrease of EA from V_2O_6 to V_2O_7 (Table I). The singly occupied HOMO of the $V_2O_7^-$ anion is delocalized over all the oxygen atoms, but has larger contributions from the bridging oxygen atoms than the terminal or peroxo ones, which is in contrast to that for $V_2O_6^-$.[21] Again, all the observed PES features [Fig. 4(b)] can be straightforwardly assigned to photodetachment of electrons from oxygen $2p$-derived orbitals.

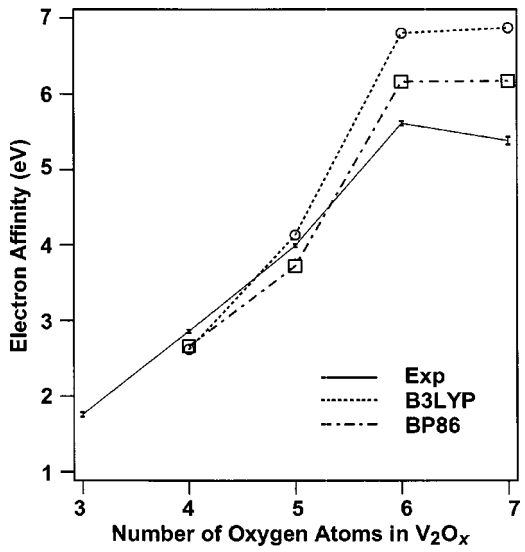

FIG. 6. Measured electron affinities for V_2O_x ($x=3-7$) (solid line with error bars) as a function of oxygen content. DFT results for V_2O_x ($x=4-7$) at B3LYP (open circle) and BP86 (open square) levels of theory from Ref. 21 are also plotted for comparison.

6. Sequential oxidation

A trend of sequential oxidation is clearly observed from Fig. 5(a) with increasing oxygen content. The PES spectra for $V_2O_x^-$ gradually shifted to higher binding energies from $x=3$ to 5. Then a dramatic PES pattern change is observed from $x=5$ to 6. This is because for $V_2O_x^-$ ($x=3-5$) the low-binding-energy features are all due to $3d$-derived orbitals. For the oxygen-excess $V_2O_6^-$ and $V_2O_7^-$ clusters, all vanadium $3d$ electrons are transferred to oxygen and their valence molecular orbitals are dominated by oxygen $2p$ orbitals, which have very high binding energies (>5 eV), as labeled in Fig. 5(a). Thus the PES data revealed how the electronic properties and chemical bonding in the divanadium oxide clusters evolve with increasing oxygen content, showing a clear picture of sequential oxidation.

B. Comparison of experimental and theoretical electron affinities

The well-defined and sharp onset of the threshold PES feature allowed us to obtain fairly accurate electron affinities for the corresponding neutral oxide species, as given in Table I. Vyboishchikov and Sauer[21] calculated the EA's for V_2O_x ($x=4-7$) using DFT at B3LYP and BP86 levels. The EA's for V_2O_x ($x=3-7$) as measured from the current PES experiments are shown in Fig. 6, where they are compared with the DFT results. We can see that the EA increases rapidly from $x=3$ to 6 and then slightly decreases from $x=6$ to 7. This trend is generally reproduced by the DFT results except that the EA's for $x=6$ and 7 were overestimated by 0.5–1.5 eV. The EA increases linearly with x from $x=3-5$ and then exhibits a larger step from $x=5$ to 6, reflecting the change of nature of the anion HOMO, which is primarily of $3d$ characters in $x=3-5$ and oxygen $2p$ characters in $V_2O_6^-$ and $V_2O_7^-$. The slight EA decrease from $x=6$ to 7 is likely due to the decreased degree of delocalization of the anion HOMO orbital in the latter. While the HOMO is delocalized over all six oxygen atoms with large contributions from the four terminal oxygen atoms in $V_2O_6^-$, it is delocalized over the seven oxygen atoms with large contributions from the two bridging oxygen atoms in $V_2O_7^-$.[21] It should be pointed out that the EA's of 5.61 eV for V_2O_6 and 5.38 eV for V_2O_7 are among the highest ever reported in the gas phase,[40] suggesting that neutral V_2O_6 and V_2O_7 molecules are strong oxidizers and belong to the class of high EA species called superhalogens.[41,42]

C. Vibrational structures in the spectra of $V_2O_4^-$ and $V_2O_6^-$ and further implications for their structure and bonding

A surprising observation in the current study is that the ground state PES feature (X) was vibrationally resolved for $V_2O_4^-$ and $V_2O_6^-$. A vibrational frequency of 1090 cm^{-1} was measured for V_2O_4, and 800 cm^{-1} for V_2O_6. Since only totally symmetric vibrational modes are allowed in photodetachment transitions, this observation indicates that V_2O_4 and V_2O_6 possess more symmetric structures than the other species, which is indeed the case as shown in Fig. 5(b).

In the structure of V_2O_4 [Fig. 5(b)], the bridging VO bonds can be viewed as single bonds, whereas the terminal bonds can be viewed as V═O double bonds. Since the anion HOMO is located on the two vanadium atoms, detaching the electron from the HOMO is expected to activate a totally symmetric mode involving the terminal VO stretching. This is responsible for the observed vibrational frequency of 1090 cm^{-1}, which is in excellent agreement with the previous theoretical prediction (1091 cm^{-1}) by Calatayud *et al.*[23] It should be pointed out that similar vibrational frequencies were also observed in other vanadium-oxide clusters containing V═O double bonds. In a previous PES study of monovanadium-oxide clusters, Wu and Wang reported a stretching frequency of 970 cm^{-1} for VO_2,[16] where the VO bonds were explained as double bonds. Asmis *et al.*[17] recently observed an infrared absorption band at 1032 cm^{-1} in the infrared photodissociation spectra of $V_4O_{10}^+$, which was assigned to a V═O stretching vibration.

V_2O_6 and $V_2O_6^-$ also possess highly symmetric structures [Fig. 5(b)]. Here the extra electron in the anion occupies the oxygen $2p$-derived HOMO, which is delocalized over all six oxygen atoms, but with larger contributions from the four terminal oxygen atoms. Hence photodetachment from the anion HOMO is expected to activate a mode primarily of the terminal VO stretching in V_2O_6. The terminal VO bond order in V_2O_6 can be roughly viewed as 1.5, smaller than the V═O double bonds in V_2O_4, consistent with the observed vibrational frequencies. Interestingly, a VO stretching frequency of 668 cm^{-1} was reported in infrared spectra of V_2O_2 (four-membered ring structure) in a solid argon matrix[19] where the VO bond can be viewed as a single bond. Thus our observation of a vibrational frequency of 800 cm^{-1} for V_2O_6 lies exactly in between a typical V–O single bond (668 cm^{-1}) (Ref. 19) and a typical V═O double bond (1090 cm^{-1}, Table I), in good agreement with the estimated bond order of 1.5 for the terminal VO bonds in V_2O_6. Calatayud *et al.*[23] predicted a symmetric vibrational fre-

quency of 760 cm^{-1} for V_2O_6, in reasonable agreement with our observation.

V. CONCLUSIONS

In conclusion, we report a photoelectron spectroscopic investigation of a series of divanadium-oxide clusters $V_2O_x^-$ ($x=3-7$). Well-resolved PES spectra revealed structural and electronic evolution and chemical bonding in $V_2O_x^-$ and V_2O_x. Sequential oxidation is observed up to $x=5$. In the PES spectra for $x\leqslant 5$, relatively weak and low-binding-energy features due to vanadium $3d$ electrons were observed, and the binding energies gradually increase with increasing oxygen content. A dramatic PES pattern change was observed from $V_2O_5^-$ to $V_2O_6^-$, and the PES spectra for the larger oxide clusters are characteristic of PES features of oxygen $2p$ character at very high binding energies (>5 eV). Vibrationally resolved PES spectra were observed for $V_2O_4^-$ and $V_2O_6^-$, and the observed vibrational frequencies due to VO stretching are in good agreement with previous DFT predictions. Fairly accurate electron affinities were obtained for the V_2O_x species and are compared with previous theoretical predictions. Extremely high electron affinities were observed for the oxygen-rich species V_2O_6 and V_2O_7.

ACKNOWLEDGMENTS

This research was supported by the National Science Foundation (Grant No. CHE-9817811). The experiment was performed at the W. R. Wiley Environmental Molecular Sciences Laboratory, a national scientific user facility sponsored by the DOE's Office of Biological and Environmental Research and located at Pacific Northwest National Laboratory, operated for the DOE by Battelle.

[1] C. N. R. Rao and B. Raven, *Transition Metal Oxides* (VCH, New York, 1995).
[2] I. A. Campbell, *Catalysis at Surfaces* (Chapman and Hall, New York, 1988).
[3] N. Y. Topsoe, Science **265**, 1217 (1994).
[4] B. Grzybowska-Swierkosz, Appl. Catal., A **157**, 263 (1997).
[5] G. A. Somorjai, Chem. Rev. **96**, 1223 (1996); *Introduction to Surface Chemistry and Catalysis* (Wiley, New York, 1994), pp. 402–409.
[6] R. C. Bell, K. A. Zemski, K. P. Kerns, H. T. Deng, and A. W. Castleman, Jr., J. Phys. Chem. A **102**, 1733 (1998).
[7] R. C. Bell, K. A. Zemski, and A. W. Castleman, Jr., J. Phys. Chem. A **102**, 8293 (1998).
[8] R. C. Bell, K. A. Zemski, and A. W. Castleman, Jr., J. Phys. Chem. A **103**, 2992 (1999).
[9] R. C. Bell, K. A. Zemski, and A. W. Castleman, Jr., J. Phys. Chem. A **103**, 1585 (1999).
[10] S. E. Kooi and A. W. Castleman, Jr., J. Phys. Chem. A **103**, 5671 (1999).
[11] R. C. Bell, K. A. Zemski, D. R. Justes, and A. W. Castleman, Jr., J. Chem. Phys. **114**, 798 (2001).
[12] K. A. Zemski, D. R. Justes, and A. W. Castleman, Jr., J. Phys. Chem. A **105**, 10 237 (2001).
[13] M. Foltin, G. J. Stueber, and E. R. Bernstein, J. Chem. Phys. **111**, 9577 (1999).
[14] E. B. Rudnyi, E. A. Kaibicheva, and L. N. Sidorov, J. Chem. Thermodyn. **25**, 929 (1993).
[15] A. Dinca, T. P. Davis, K. J. Fisher, D. R. Smith, and G. D. Willett, Int. J. Mass Spectrom. Ion Processes **182/183**, 73 (1999).
[16] H. Wu and L. S. Wang, J. Chem. Phys. **108**, 5310 (1998).
[17] K. R. Asmis, M. Brummer, C. Kaposta, G. Santambrogio, G. von Helden, G. Meijer, K. Rademan, and L. Wöste, Phys. Chem. Chem. Phys. **4**, 1101 (2002).
[18] L. B. Knight, Jr., R. Babb, M. Ray, T. J. Banisaukas III, L. Russon, R. S. Dailey, and E. R. Davidson, J. Chem. Phys. **105**, 10 237 (1996).
[19] G. V. Chertihin, W. D. Bare, and L. Andrews, J. Phys. Chem. A **101**, 5090 (1997).
[20] M. Calatayud, B. Silvi, J. Andres, and A. Beltran, Chem. Phys. Lett. **333**, 493 (2001).
[21] S. F. Vyboishchikov and J. Sauer, J. Phys. Chem. A **104**, 10 913 (2000).
[22] S. F. Vyboishchikov and J. Sauer, J. Phys. Chem. A **105**, 8588 (2001).
[23] M. Calatayud, J. Andres, and A. Beltran, J. Phys. Chem. A **105**, 9760 (2001).
[24] J. R. T. Johnson and I. Panas, Inorg. Chem. **39**, 3192 (2000).
[25] J. Fan, J. B. Nicholas, J. M. Price, S. D. Colson, and L. S. Wang, J. Am. Chem. Soc. **117**, 8277 (1995).
[26] L. S. Wang, J. B. Nicholas, M. Dupuis, H. Wu, and S. D. Colson, Phys. Rev. Lett. **78**, 4450 (1997).
[27] H. Wu, X. Li, X. B. Wang, C. F. Ding, and L. S. Wang, J. Chem. Phys. **109**, 449 (1998).
[28] H. Wu, S. R. Desai, and L. S. Wang, J. Am. Chem. Soc. **118**, 5296 (1996).
[29] L. S. Wang, H. Wu, and S. R. Desai, Phys. Rev. Lett. **76**, 4853 (1996).
[30] L. S. Wang, H. Wu, S. R. Desai, and L. Lou, Phys. Rev. B **53**, 8028 (1996).
[31] H. J. Zhai, X. Yang, X. B. Wang, L. S. Wang, B. Elliott, and A. I. Boldyrev, J. Am. Chem. Soc. **124**, 6742 (2002).
[32] L. S. Wang, in *Photoionization and Photodetachment*, Vol. 10 of *Advanced Series in Physical Chemistry*, edited by C. Y. Ng (World Scientific, Singapore, 2000), pp. 854–957.
[33] L. S. Wang, H. S. Cheng, and J. Fan, J. Chem. Phys. **102**, 9480 (1995).
[34] L. S. Wang and H. Wu, in *Cluster Materials*, Vol. 4 of *Advances in Metal and Semiconductor Clusters*, edited by M. A. Duncan (JAI, Greenwich, 1998), pp. 299–343.
[35] F. A. Cotton and G. Wilkinson, *Advanced Inorganic Chemistry*, 5th ed. (Wiley, New York, 1988).
[36] C. W. Bauschlicher, Jr. and P. Maitre, Theor. Chim. Acta **90**, 189 (1985).
[37] C. W. Bauschlicher, Jr. and S. R. Langhoff, J. Chem. Phys. **85**, 5936 (1986).
[38] M. Dolg, U. Wedig, H. Stoll, and H. Preuss, J. Chem. Phys. **86**, 2123 (1987).
[39] E. G. Bakalbassis, M. D. Stiakaki, A. C. Tsipis, and C. A. Tsipis, Chem. Phys. **205**, 389 (1996).
[40] J. C. Rienstra-Kiracofe, G. S. Tschumper, H. F. Schaefer III, S. Nandi, and G. B. Ellison, Chem. Rev. **102**, 231 (2002).
[41] G. L. Gutsev and A. I. Boldyrev, Adv. Chem. Phys. **61**, 169 (1985).
[42] X. B. Wang, C. F. Ding, L. S. Wang, A. I. Boldyrev, and J. Simons, J. Chem. Phys. **110**, 4763 (1999).